

RESEARCH LETTER

10.1002/2018GL077628

Key Points:

- Lightning 3-D mapping with high accuracy and great details has been realized by the Fast Antenna Lightning Mapping Array (FALMA)
- Stepped leaders with multiple branches, K changes, and dart leaders with speeds up to 2.4×10^7 m/s are well imaged
- Horizontal location accuracy is estimated to be around 20 m by comparing locations of successive return strokes in CG flashes

Supporting Information:

- Supporting Information S1
- Movie S1
- Movie S2
- Movie S3
- Movie S4
- Movie S5
- Movie S6
- Movie S7

Correspondence to:

T. Wu,
tingwu@gifu-u.ac.jp

Citation:

Wu, T., Wang, D., & Takagi, N. (2018). Lightning mapping with an array of fast antennas. *Geophysical Research Letters*, 45, 3698–3705. <https://doi.org/10.1002/2018GL077628>

Received 20 FEB 2018

Accepted 21 MAR 2018

Accepted article online 26 MAR 2018

Published online 16 APR 2018

Lightning Mapping With an Array of Fast Antennas

Ting Wu¹ , Daohong Wang¹ , and Nobuyuki Takagi¹

¹Department of Electrical, Electronic and Computer Engineering, Gifu University, Gifu, Japan

Abstract Fast Antenna Lightning Mapping Array (FALMA), a low-frequency lightning mapping system comprising an array of fast antennas, was developed and established in Gifu, Japan, during the summer of 2017. Location results of two hybrid flashes and a cloud-to-ground flash comprising 11 return strokes (RSs) are described in detail in this paper. Results show that concurrent branches of stepped leaders can be readily resolved, and K changes and dart leaders with speeds up to 2.4×10^7 m/s are also well imaged. These results demonstrate that FALMA can reconstruct three-dimensional structures of lightning flashes with great details. Location accuracy of FALMA is estimated by comparing the located striking points of successive RSs in cloud-to-ground flashes. Results show that distances between successive RSs are mainly below 25 m, indicating exceptionally high location accuracy of FALMA.

Plain Language Summary We have developed a lightning mapping system called Fast Antenna Lightning Mapping Array (FALMA). FALMA detects low-frequency radio waves produced by lightning discharges at multiple sites and can reconstruct 3-D structures of lightning flashes. Three lightning flashes are analyzed in detail in this paper, and animations of seven cases are provided in the supporting information. These results demonstrate that FALMA can show development of lightning discharges in great details and accuracy. Types and polarities of lightning discharges can also be determined by the recorded electric field change waveforms. FALMA is expected to become a unique tool for lightning and thunderstorm researches. Research studies of several topics are already underway based on the observation data in the summer of 2017.

1. Introduction

Lightning discharges produce a wideband of electromagnetic radiation, among which radio waves are widely used for ground-based lightning locating. Depending on different purposes, various frequency ranges of radio waves are utilized in different lightning locating systems. Well-known lightning locating systems include, among others, the World Wide Lightning Location Network (e.g., Rudlosky & Shea, 2013), which detects very low-frequency radio waves; the U.S. National Lightning Detection Network (e.g., Cummins & Murphy, 2009), which operates in very low frequency and low-frequency (LF) bands; and the Lightning Mapping Array (LMA) (Rison et al., 1999) working in the very high frequency (VHF) band.

Most operational lightning locating systems can only do two-dimensional (2-D) locating, which is sufficient for most practical purposes such as locating lightning-caused damages. However, for research purposes, especially those involving lightning channel development, lightning initiation, and thunderstorm charge structures and so on, height information and detailed three-dimensional (3-D) structures of lightning discharges are necessary. The most successful 3-D lightning locating system is the LMA. As a VHF system, the location accuracy of the LMA is about 6 to 12 m in the horizontal direction and 20 to 30 m in the vertical direction for sources over the network (Thomas et al., 2004). Detailed 3-D structures of lightning flashes can be mapped with the LMA, which has significantly facilitated lightning and thunderstorm research studies.

In recent years, 3-D locating in the LF band is rapidly developing (Bitzer et al., 2013; Karunarathne et al., 2013; Yoshida et al., 2014). The major advantage of observations in the LF band is that the recorded electric field change (E-change) waveforms can be used to determine discharge types, polarities, and to infer currents. However, compared to VHF systems, the location accuracy is generally lower, and sources that can be located are much fewer. Recent studies by Lyu et al. (2014, 2016) made significant improvements on LF 3-D mapping by using a hybrid interferometric-time of arrival (TOA) technique combined with a continuous data recording scheme. They reported that thousands of sources can be located for a typical lightning flash by their five-station magnetic sensors.

Due to the valuable waveform information, an LF system with a high 3-D mapping capability can be even more useful as a lightning research tool than VHF systems. In this paper, we will introduce our newly

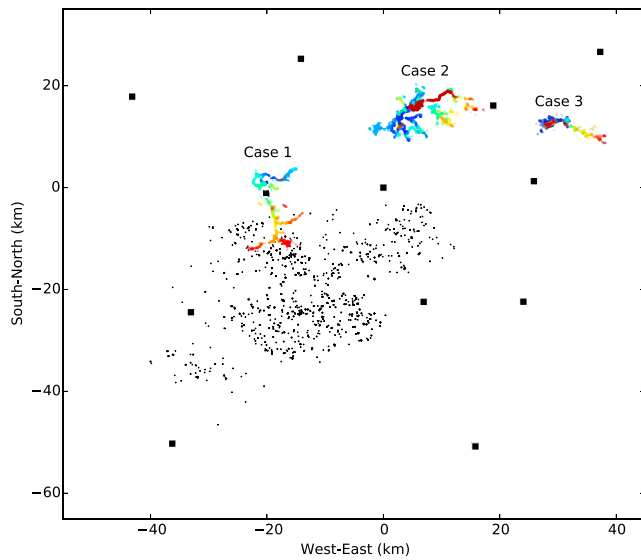


Figure 1. Network of Fast Antenna Lightning Mapping Array during the summer observation in 2017. The black squares represent 12 sites. The latitude and longitude of the site at (0, 0) is (35.475°E, 136.960°N). Sources of three lightning flashes described in section 3 are also plotted. The black dots represent locations of return strokes analyzed in section 4.

developed LF lightning locating system called Fast Antenna Lightning Mapping Array (FALMA). As the name suggests, it is a system comprising an array of fast antennas. This paper serves as a prompt report based on the observation in the summer of 2017 to show the capability of FALMA to do exceptionally detailed 3-D mapping with high accuracy and demonstrate that LF systems are indeed capable of 3-D mapping similar to the LMA operating in the VHF band.

2. Experiment and Methods

FALMA is a system consisting of multiple sites of fast antennas. During its observation in the summer of 2017, 12 sites were set up. Figure 1 shows the network, which covers an area of about $90 \times 90 \text{ km}^2$. The distances between neighboring sites are about 20 to 30 km. At each site, there is a fast antenna, an AD converter, a computer, and some devices for internet connection. All sites are synchronized with Global Positioning System.

The fast antenna is a flat plate antenna similar in principle to that described by Kitagawa and Brook (1960). It has a time constant of 200 μs and records radio waves in the frequency band of about 500 Hz to 500 kHz. The AD converter has a resolution of 16 bits. In order to achieve a timing accuracy as high as possible, we use a sampling rate of 25 MS/s. The recording length of each trigger is 1 s with a pretrigger length of 100 ms. Full waveform data are recorded for post processing.

A lot of efforts have been made to overcome shortcomings of an LF system and to achieve location results as good as a VHF system. Features of FALMA that are important for improving the performance of 3-D mapping are described as follows.

2.1. High Sensitivity of the Fast Antenna

Fast antennas of FALMA were newly designed and manufactured. Fast antennas with various structures were tested. They were set up at the same location, and signals from the same lightning discharges were compared to find out the structure with the highest signal-to-noise ratio (SNR). For example, our tests indicate that antennas with upward facing flat plates generally have a higher SNR than those with downward facing flat plates. A higher SNR means that more pulses can emerge from the background noise and be located, contributing to a more complete image of reconstructed lightning channels.

2.2. High Timing Accuracy

A sampling rate of 25 MS/s is used for FALMA, corresponding to the timing accuracy of 40 ns. As the timing accuracy of Global Positioning System is about 40 to 50 ns, 25 MS/s is the highest meaningful sampling rate. Although the effective timing error for location will not be as small as 40 ns due to the limited analog bandwidth, sampling at 25 MS/s minimizes timing uncertainty as much as possible.

2.3. Continuous Data Recording Capability

Normally during the period when the triggered data are being written to the hard drive, new signals cannot be processed and are lost, and the so-called “dead time” arises. The dead time problem is especially serious when the sampling rate is high and the data recording length is long. In order to solve the dead time problem, we developed a new recording scheme by fully utilizing the computer memory. When there comes a trigger and the triggered data are being written to the hard drive, the input data from the AD converter are temporarily stored in the memory and are processed after the writing of the triggered data is finished. In this way, all waveform data can be fully recorded. This is especially important when a flash lasts for a long time. Similarly, the improvement made by Stock et al. (2014) on VHF interferometry was primarily due to the continuous recording capability.

2.4. Waveform Correlation for Pulse Matching

FALMA uses the TOA method for 3-D locating. The most difficult part in the TOA method is accurately matching pulses recorded at different sites. Since every site of FALMA records the full waveform, it is preferable to use waveform correlation to match pulses at different sites, which is more accurate and efficient than purely trying different combinations. The waveform correlation method was also used by Lyu et al. (2014) in their interferometric-TOA technique, which largely improved location results of their LF system.

2.5. Relatively High-Frequency Band for Locating

The frequency band of the recorded waveform is about 500 Hz to 500 kHz. However, it is not necessary to use the full bandwidth for locating; it is more advantageous to use a relatively high frequency part for locating. Frequency is directly related with the spatial scale of the discharge, so higher frequency components can theoretically yield location results with higher accuracy. Moreover, a narrower frequency band means many noise signals can be excluded, and more pulses produced by lightning discharges can be detected and located. FALMA uses a frequency band of 200 to 500 kHz for locating.

3. Location Results

In this section, we will describe location results of three flashes in detail. E-change waveforms, which use the atmospheric sign convention, are also provided, but as the fast antenna has not been calibrated, the waveform magnitude is not shown. Animations of the second example and six more flashes are provided as Movies S1–S7 in the supporting information to give a visual demonstration of the 3-D mapping capability of FALMA.

3.1. A Bolt-From-the-Blue Type Hybrid Flash

The first case is a bolt-from-the-blue type hybrid flash (e.g., Krehbiel et al., 2008) started as a typical intracloud (IC) flash and produced a return stroke (RS) at the end. This flash lasted for 423.3 ms, and a total of 2,880 sources were located. Figure 2 shows the waveform and 3-D location results.

The first half of this flash looks like a typical IC flash. It started with an upward negative leader, forming an almost vertical channel, presumably between the main negative charge layer and the upper positive charge layer. The vertical channel is dark blue sources and is labeled as “a” in Figure 2. The speed of the initial upward propagation is about 7.1×10^5 m/s. The upward negative leader then turned to a horizontal direction and propagated to the north before it split to two branches, which are labeled as “b1” and “b2.” The branch b2 developed to the east. Its altitude decreased from about 10 to 8 km and at last it developed almost vertically back to about 10 km. The final vertical propagation is labeled as “c.” From the E-change waveform, we can determine that this is also a negative leader. The speed of the upward propagation c is about 1.1×10^5 m/s.

The branch b1 developed to the west and soon turned to the south. It progressed for more than 10 km and had at least four clear branches labeled as d1–d4. The branch d4 turned to the ground and produced an RS. The speed of the downward negative leader appeared to increase as it approached to the ground. The overall speed is about 1.3×10^5 m/s, typical for a stepped leader.

While branches b1 and b2 were developing from the top of the initial vertical channel a, some sources were also located from the bottom of the vertical channel. According to the bidirectional leader concept (e.g., Mazur et al., 2013), as the initial negative leader develops upward, a positive leader develops in the opposite direction. In Figure 2 we can see some scattered sources at the height of about 6 km. These sources are probably produced from the main negative charge layer. They may be produced by the positive leader or recoil leaders traveling from the head of the positive leader back to the origin.

3.2. A Hybrid Flash With Multiple K Changes

The second case is shown in Figure 3. It is also a hybrid flash, but it is different from the first case in that the IC processes and the RS are initiated by different leaders. This type of hybrid flash has also been analyzed by Lu et al. (2012). Animation of this flash is provided as Movie S3 in the supporting information.

This flash started with a succession of negative leaders propagating upward from the main negative charge region, but all of them stopped developing before forming typical horizontal propagations in the upper positive charge region. At the time of about 300 ms, a downward stepped leader was formed and it produced an

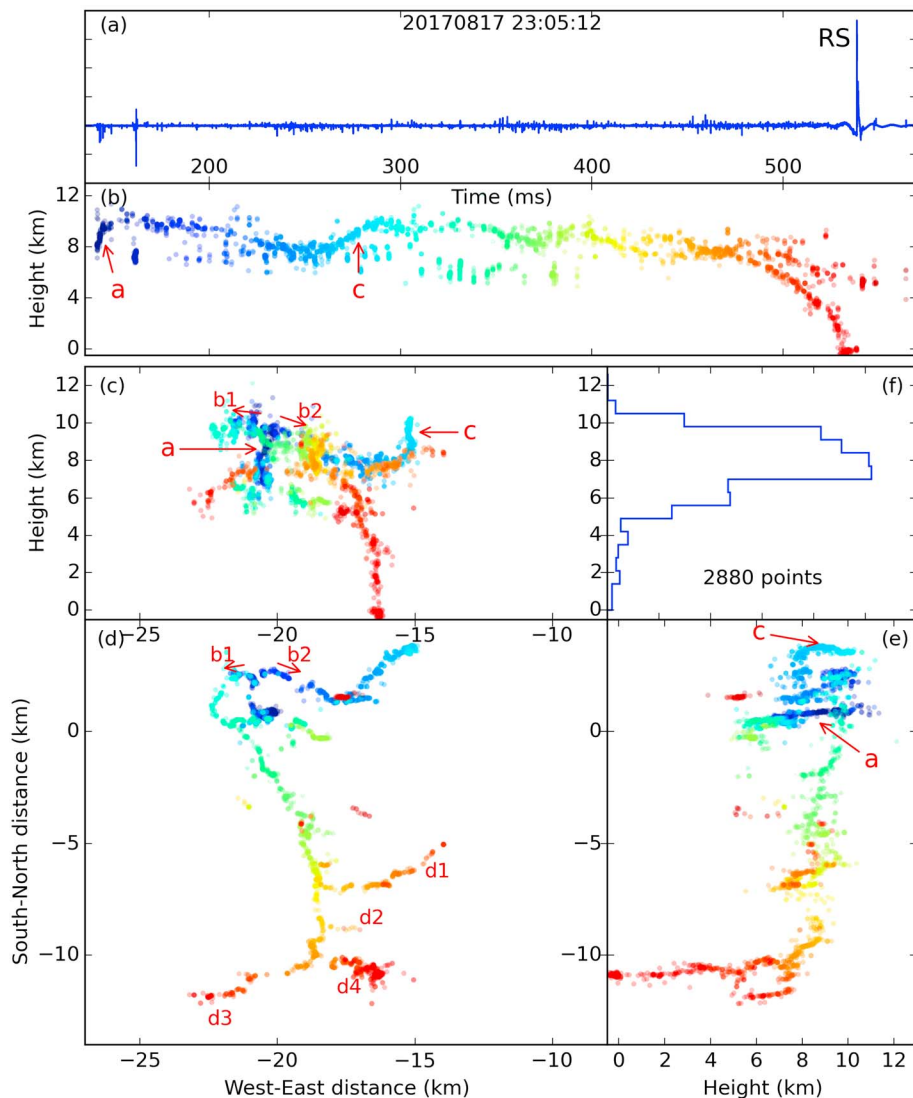


Figure 2. E-change waveform and 3-D location results of case 1 in Figure 1. (a) E-change waveform. (b) Height-time view. (c) Height-distance (from west to east) view. (d) Plan view. (e) Distance (from south to north)-height view. (f) Source distribution along the height. The color scale indicates the time corresponding to the time coordinate of Figure 2b.

RS. From Movie S3, we can see that the downward leader was initiated from the head of an old channel that had stopped developing. From Figures 2c and 2e we can see that the downward leader had at least three branches traveling simultaneously. All of them reached very close to the ground but only one successfully touched the ground and produced an RS (cross sign).

After the RS, five K changes were clearly imaged and labeled as k1–k5 in Figure 3b. From Figures 3c and 3e, sources from k1–k4 cannot be seen as they are completely covered by sources of k5. This feature also indicates the high location accuracy of FALMA.

3.3. A Negative Cloud-to-Ground Flash Comprising 11 RSs

The third example is a negative cloud-to-ground (CG) flash comprising 11 RSs as shown in Figure 4. Each panel in Figure 4 shows the location results in height-time view along with E-change waveforms. Eleven RSs are labeled as R1–R11. Sources of this flash are also plotted in Figure 1 and labeled as “Case 3.”

This flash started with a direct downward propagation as shown in Figure 4b. Normally, a CG flash starts with the preliminary breakdown and followed by a stepped leader. In this case, there is no clear boundary

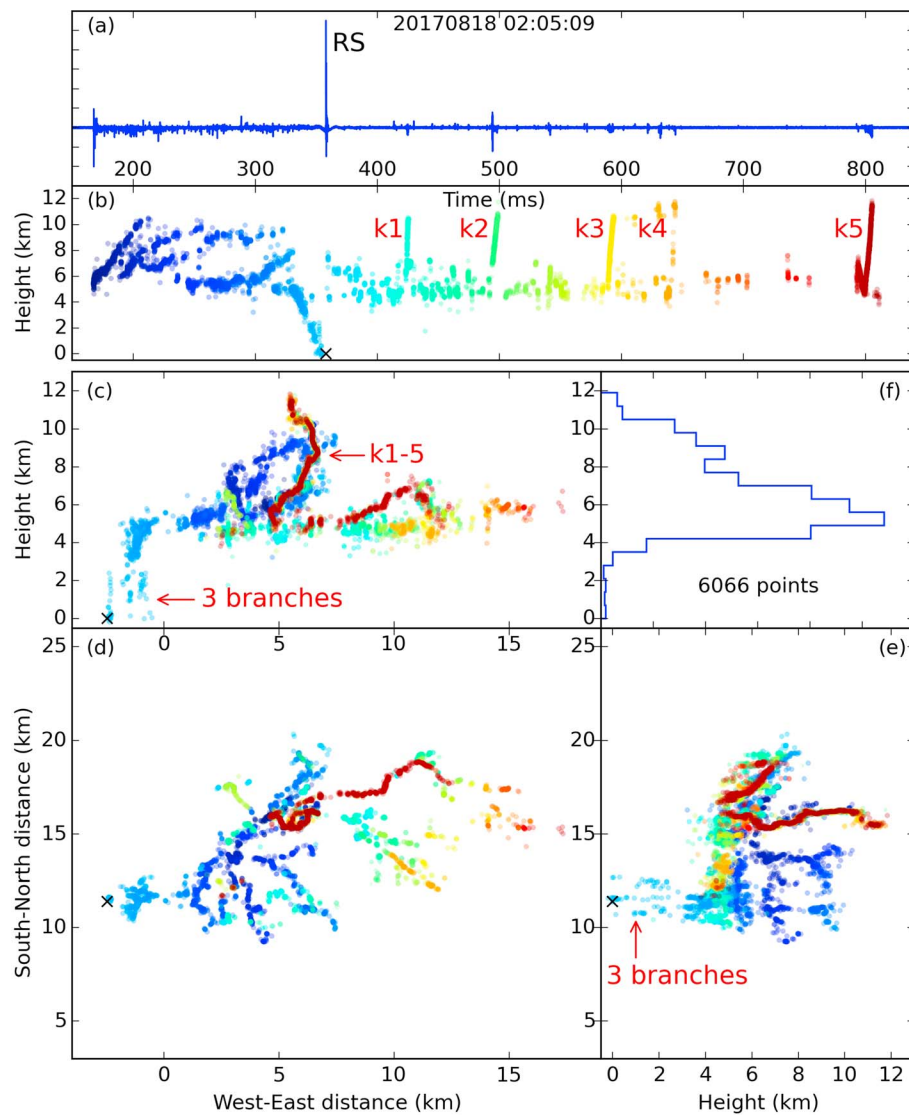


Figure 3. (a-f) E-change waveform and 3-D location results of case 2 in Figure 1. Subplots are arranged as in Figure 2. The cross sign indicates the return stroke (RS).

between the preliminary breakdown and the stepped leader, and for simplicity, the whole processes before R1 are considered as one stepped leader. The speed of the stepped leader is about 2.0×10^5 m/s. A few sources (dark red) are also located for the RS R1.

The second RS R2 occurred about 187 ms after R1. About 10 ms before R2, a K change was located as shown in Figure 4c. This K change reached very close to the ground, but actually, it did not reach the ground. According to the E-change waveform, there was no RS at the end of this K change and this K change had no direct connection with R2. Therefore, this K change may also be called "attempted leader" (Rhodes et al., 1994), which is a dart leader that does not reach the ground. This K change was clearly imaged, and its overall speed was about 2.6×10^6 m/s. This example shows the importance of the E-change waveform data in identifying discharge processes. Without the waveform, this K change could be easily misinterpreted as a dart leader reaching the ground.

Subsequent RSs (R2-R11) occurred with time intervals of 25 to 60 ms. Leaders before these RSs were all located, four of which are shown in Figures 4d-4g. All of these leaders seem to be dart leaders. The dart leader in Figure 4d had a large speed of 2.4×10^7 m/s. Probably because of its large speed, only a few sources were located. The speed for leaders in Figures 4e-4g ranged from 5.5 to 8.1×10^6 m/s. These leaders were all well located.

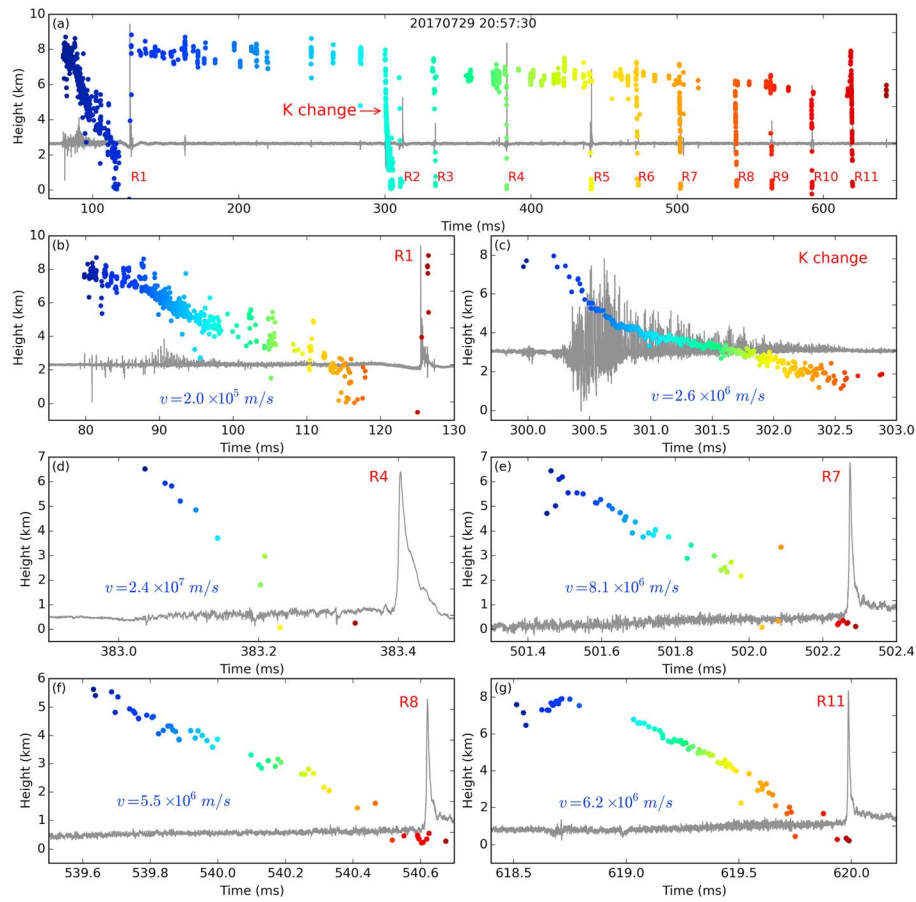


Figure 4. (a–g) E-change waveform and location results of a negative cloud-to-ground flash comprising 11 return strokes. Each subplot is shown in height-time view with the color scale indicating time. Figures 4b–4g are some enlarged portions in Figure 4a.

We can notice one problem from the results that when a leader gets close to the ground, location results seem to be more scattered. This is a common problem that the location accuracy for discharges with a low altitude is relatively low. One possible reason is that radio waves produced by discharges near the ground are easily affected by the lossy ground and the topography when propagating to observation sites.

From Figure 4a we can also see that some sources are located at the height of 6 to 9 km throughout this flash. This indicates that the main negative charge layer is at the height of 6 to 9 km and all RSs are produced from this negative charge layer.

Lyu et al. (2014) reported that their LF system could also locate dart leaders in CG flashes, but the dart leaders reported by them had the downward speed of 0.8 to 2×10^6 m/s. Lyu et al. (2016) also located dart leaders in IC flashes with a speed range of 0.9 to 7.1×10^6 m/s. To our best knowledge, no LF system has ever reported locating of dart leaders with the speed on the order of 10^7 m/s.

4. Estimation of Location Accuracy Using Multistroke Lightning Flashes

In this analysis, we will evaluate the location accuracy of FALMA by comparing the distances between different RSs in CG flashes. For most CG flashes producing multiple RSs, these RSs strike at the same point. However, the location results of these RSs always have some differences due to location uncertainties. Because different RSs are independently located, differences of their locations can indicate the location accuracy of the system. Based on this principle, we located a large amount of RSs produced in a thunderstorm over the network. For every RS, the first RS that follows it is found out, and if their time difference is

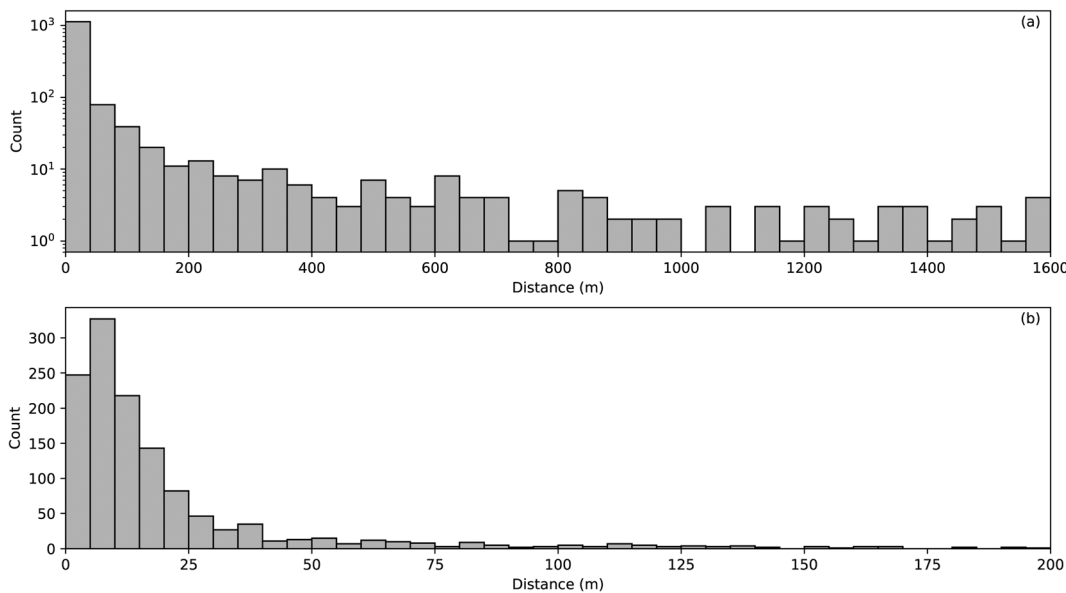


Figure 5. (a and b) Distribution of the distance between successive RSs. The y axis in Figure 5a is in the logarithmic scale.

less than 500 ms, their horizontal distance is calculated. As an example, for the CG flash in Figure 4, which contains 11 RSs, distances between i th and $(i + 1)$ th RSs ($1 \leq i \leq 10$) are calculated and 10 results are obtained. A total of 1684 results are obtained, and locations of contributing RSs are plotted as black dots in Figure 1.

The distribution of the calculated distances is shown in Figure 5. Figure 5a shows in the range of 0 to 1,600 m and Figure 5b in the range of 0 to 200 m. Note that the y axis of Figure 5a is shown in the logarithmic scale. The distance between successive RSs has a very wide distribution. The main reason is that some CG flashes have multiple ground terminations. As reported by Valine and Krider (2002), 35% CG flashes had two or more striking points separated by tens of meters or more. Another reason is that some successive RSs are actually produced in different CG flashes. Results below 200 m are replotted in Figure 5b. There are 1,274 results below 200 m, accounting for 75.7% of all results. We can see that the majority of results are smaller than 25 m. For simplicity, here we consider that all results below 200 m are due to location uncertainties. The mean value and median value of these results are 20.9 and 11.0 m, respectively, and 79.8% of these results are below 25 m.

This result indicates the high accuracy of about 20 m, at least for RSs. However, this method may not be able to evaluate systematic errors. For example, multiple RSs in a CG flash are located very close to each other, but they may be all located away from the real striking point due to certain systematic errors. We will try to do a more comprehensive analysis on the location accuracy in the future.

5. Conclusions

The capability of lightning 3-D mapping by FALMA is demonstrated in this paper. Different from traditional lightning mapping in the VHF band, FALMA uses an array of fast antennas to sense lightning radiation signals in the LF band. Location results of three lightning flashes are described in detail to demonstrate the 3-D mapping capability of FALMA. Animations of seven flashes are provided in the supporting information. Due to many improvements on both the hardware and software, FALMA can map 3-D structures of various types of lightning flashes in high accuracy and great details, representing a new level of lightning mapping capability for LF systems.

As an LF system, FALMA records the full E-change waveforms at every site. By combining waveforms and 3-D location results, we can unambiguously determine discharge types and leader polarities. It is also possible to infer discharge currents and thunderstorm charge structures. FALMA can be expected to become a unique tool for lightning and thunderstorm researches.

Acknowledgments

This work was supported by the Ministry of Education, Culture, Sports, Science, and Technology of Japan (grants 15H02597 and 16H04315). Location results used in this paper can be downloaded at <https://doi.org/10.5281/zenodo.1202489>. More examples of lightning flashes imaged by FALMA can be found at <https://www1.gifu-u.ac.jp/~lrg/falma.html>. The authors thank two anonymous reviewers for their constructive comments.

References

Bitzer, P. M., Christian, H. J., Stewart, M., Burchfield, J., Podgorny, S., Corredor, D., et al. (2013). Characterization and applications of VLF/LF source locations from lightning using the Huntsville Alabama Marx Meter Array. *Journal of Geophysical Research: Atmospheres*, 118, 3120–3138. <https://doi.org/10.1002/jgrd.50271>

Cummins, K. L., & Murphy, M. J. (2009). An overview of lightning locating systems: History, techniques, and data uses, with an in-depth look at the U.S. NLDN. *IEEE Transactions on Electromagnetic Compatibility*, 51(3), 499–518. <https://doi.org/10.1109/TEMC.2009.2023450>

Karunarathne, S., Marshall, T. C., Stolzenburg, M., Karunarathne, N., Vickers, L. E., Warner, T. A., & Orville, R. E. (2013). Locating initial breakdown pulses using electric field change network. *Journal of Geophysical Research: Atmospheres*, 118, 7129–7141. <https://doi.org/10.1002/jgrd.50441>

Kitagawa, N., & Brook, M. (1960). A comparison of intracloud and cloud-to-ground lightning discharges. *Journal of Geophysical Research*, 65, 1189–1201. <https://doi.org/10.1029/JZ065i004p01189>

Krehbiel, P. R., Riousset, J. A., Pasko, V. P., Thomas, R. J., Rison, W., Stanley, M. A., & Edens, H. E. (2008). Upward electrical discharges from thunderstorms. *Nature Geoscience*, 1(4), 233–237. <https://doi.org/10.1038/ngeo162>

Lu, G., Cummer, S. A., Blakeslee, R. J., Weiss, S., & Beasley, W. H. (2012). Lightning morphology and impulse charge moment change of high peak current negative strokes. *Journal of Geophysical Research*, 117, D04212. <https://doi.org/10.1029/2011JD016890>

Lyu, F., Cummer, S. A., Lu, G., Zhou, X., & Weinert, J. (2016). Imaging lightning intracloud initial stepped leaders by low-frequency interferometric lightning mapping array. *Geophysical Research Letters*, 43, 5516–5523. <https://doi.org/10.1002/2016GL069267>

Lyu, F., Cummer, S. A., Solanki, R., Weinert, J., McTague, L., Katko, A., et al. (2014). A low-frequency near-field interferometric-TOA 3-D Lightning Mapping Array. *Geophysical Research Letters*, 41, 7777–7784. <https://doi.org/10.1002/2014GL061963>

Mazur, V., Ruhnke, L. H., Warner, T. A., & Orville, R. E. (2013). Recoil leader formation and development. *Journal of Electrostatics*, 71(4), 763–768. <https://doi.org/10.1016/j.elstat.2013.05.001>

Rhodes, C. T., Shao, X. M., Krehbiel, P. R., Thomas, R. J., & Hayenga, C. O. (1994). Observations of lightning phenomena using radio interferometry. *Journal of Geophysical Research*, 99, 13,059–13,082. <https://doi.org/10.1029/94JD00318>

Rison, W., Thomas, R. J., Krehbiel, P. R., Hamlin, T., & Harlin, J. (1999). A GPS-based three-dimensional lightning mapping system: Initial observations in central New Mexico. *Geophysical Research Letters*, 26, 3573–3576. <https://doi.org/10.1029/1999GL010856>

Rudlosky, S. D., & Shea, D. T. (2013). Evaluating WWLLN performance relative to TRMM/LIS. *Geophysical Research Letters*, 40, 2344–2348. <https://doi.org/10.1002/grl.50428>

Stock, M. G., Akita, M., Krehbiel, P. R., Rison, W., Edens, H. E., Kawasaki, Z., & Stanley, M. A. (2014). Continuous broadband digital interferometry of lightning using a generalized cross-correlation algorithm. *Journal of Geophysical Research: Atmospheres*, 119, 3134–3165. <https://doi.org/10.1002/2013JD020217>

Thomas, R. J., Krehbiel, P. R., Rison, W., Hunyady, S. J., Winn, W. P., Hamlin, T., & Harlin, J. (2004). Accuracy of the Lightning Mapping Array. *Journal of Geophysical Research*, 109, D14207. <https://doi.org/10.1029/2004JD004549>

Valine, W. C., & Krider, E. P. (2002). Statistics and characteristics of cloud-to-ground lightning with multiple ground contacts. *Journal of Geophysical Research*, 107(D20), 4441. <https://doi.org/10.1029/2001JD001360>

Yoshida, S., Wu, T., Ushio, T., Kusunoki, K., & Nakamura, Y. (2014). Initial results of LF sensor network for lightning observation and characteristics of lightning emission in LF band. *Journal of Geophysical Research: Atmospheres*, 119, 12,034–12,051. <https://doi.org/10.1002/2014JD022065>